Physica A 540 (2020) 123055

Contents lists available at ScienceDirect

Physica A

journal homepage: www.elsevier.com/locate/physa

Percolation of new products

Gadi Fibich, Tomer Levin *

Department of Applied Mathematics, School of Mathematical Sciences, Tel Aviv University, Tel Aviv 6997801, Israel

ARTICLE INFO

Article history:
Received 11 June 2019
Received in revised form 2 October 2019
Available online 25 October 2019

MSC:
60K35
90B60
91B99
92D25

Keywords:
Diffusion
New product
Percolation
Phase transition
Bass model

ABSTRACT

In most models of diffusion of new products, every individual in the social network is a potential adopter. When, however, a fraction α of the individuals cannot adopt the product at any time, the new product percolates (rather than diffuses) in the network, similarly to movement through porous materials. We obtain explicit expressions for the fraction of adopters as a function of time, for complete networks, circular networks, D-dimensional Cartesian networks, small-worlds networks, and scale-free networks. These expressions show that the complex effect of percolation can be captured by two simple aggregate effects: Decreasing the market potential by $1-\alpha$, and reducing the peers effect by $(1-\alpha)^k$, where k depends on the network type. Hence, percolation of new products is qualitatively similar to diffusion of new products. In particular, there is no threshold value at which a phase transition occurs.

1. Introduction

Diffusion of new products is a classical problem in marketing [1]. The diffusion begins as the new product is introduced into a market, and progresses through a series of adoption events. The first mathematical model for product diffusion was formulated in 1969 by Bass [2], and it inspired hundreds of theoretical studies [3]. Unlike epidemiological models, most of these studies have not been on whether the new product will spread out, but rather on the rate at which it would do so (e.g., the time to reach 50% of its market potential). Despite the huge body of research on the Bass model, there is still a limited understanding of the effect of the network structure on the diffusion [4].

The motivation for this study comes from the diffusion of residential rooftop solar PV systems, which received a considerable interest in recent years [5–8]. Since the key predictor of installing a solar panel is having a neighbor who already installed one [9,10], the relevant network for solar systems is a two-dimensional Cartesian grid, where each node corresponds to a residential unit. Diffusion on two-dimensional Cartesian grids was studied in [4]. That study, however, did not take into account that a considerable fraction (up to 40%) of the residential units are inappropriate for installation of a solar system (since the roof is too small, it does not get sufficient sunlight, etc.). More broadly, nearly all the literature on diffusion of new products assumed that everyone in the market is a potential adopter. This is not the case, however, not only for solar systems, but also for products that can only be adopted by individuals below a certain age, above a certain annual income, of a certain gender, who own a car, who speak a certain language, etc. In such cases, the product percolates (rather than diffuses) through the social network.[1] The goal of this paper is to study how the change from diffusion to percolation affects the aggregate adoption of the new product.

* Corresponding author.
E-mail address: tomerlevin1@mail.tau.ac.il (T. Levin).

[1] The few studies in the literature on percolation of new products used a different modeling approach, and therefore reached very different conclusions (see Section 1.1).

https://doi.org/10.1016/j.physa.2019.123055
0378-4371/

Our analysis and simulations show that "removing" a fraction α of the population from participating in the diffusion process reduces both the market potential and the rate at which this market potential is reached. Specifically, the market potential decreases by $1-\alpha$, and the peers influence parameter q decreases by $(1-\alpha)^k$, where k depends on the network type, see (1). Hence, the "removal" of nodes does not have a qualitative effect on the aggregate adoption. In particular, in percolation of new products, there is no threshold value for the product to be successful (i.e., to reach its entire market potential).

1.1. Literature review

The first quantitative percolation model in marketing was introduced by Solomon et al. [11] and Weisbuch and Stauffer [12] in order to analyze hits and flops in the movie industry. They considered the diffusion of a new movie of quality v through heterogeneous individuals that are positioned on a square lattice. A "hit" is reported if there exists a path of individuals for which $u_i > v$ that touches all borders of the lattice, where u_i is the preference of individual i. Otherwise, a "flop" is reported. This percolation model showed the existence of a threshold value for the movie quality v between hits and flops. Subsequent studies extended this model to higher-dimensional Cartesian grids [13] and scale-free networks [14]. Learning effects (such as reducing the product price with the cumulative quantity of units already produced) were added by Hohnisch et al. [15], and by Cantono and Silverberg [16] for percolation of environmental-friendly energy technologies.

In all of the above quantitative studies of percolation of new products, the agent-based models shared two assumptions:

A1. The diffusion originated from several early buyers ("early birds") at time $t = 0$.
A2. All subsequent adoptions only occurred through peers effect.

These assumptions are common in percolation models, and are used e.g., in epidemiology to model the spread of diseases in a partially-immunized society (i.e., the Susceptible–Infected (SI) model of epidemics [17]). In agent-based Bass models of diffusion of new products, however, different assumptions are usually used (see e.g. [4,18,19]):

A1*. Initially ($t = 0$), all consumers are non-adopters.
A2*. Subsequent adoptions can occur as a result of both peers effect and external influences (mass media, commercials, etc.).

As discussed in [4,20], this change in the model assumptions has a dramatic effect on the diffusion, even without nodes removal. Indeed, diffusion in SI-type models depends on global properties of the network (connectivity, size of giant component, average distance between nodes), whereas diffusion in the Bass model depends on local properties of the network (e.g., grid dimension). This difference explains, e.g., why the addition of a small-world structure has a large effect on the spread of epidemics but a negligible effect on diffusion of new products [4].

Hence, in this study we model product percolation using Assumptions A1* and A2*, rather than A1 and A2. Consequently, our results on percolation of new products are very different from those obtained in the previous studies mentioned earlier. In particular, whereas those studies predicted a threshold for the product to reach its entire market potential, no such threshold exists in our model.

The rest of the paper is organized as follows. Section 2 presents the percolation model. In Sections 3 and 4 we explicitly compute the fraction of adopters as a function of time for percolation in complete and circular networks, respectively. In Sections 5–8, we obtain explicit approximations for percolation in D-dimensional Cartesian, small-world, scale-free, and next-nearest neighbor networks, respectively. The Discussion in Section 9 focuses on the absence of a phase transition.

2. Percolation model

We model the diffusion of new products using the discrete Bass model [4]. A new product is introduced at time $t = 0$ to a market with M consumers. Initially all consumers are non-adopters. If a consumer adopts the product, she remains so at all later times. The consumers belong to a social network which is described by a graph with M nodes. If j did not adopt the product by time t, her probability to adopt it in $(t, t+\Delta t)$ is

$$\text{Prob}\begin{pmatrix} j \text{ adopts in} \\ (t, t+\Delta t) \end{pmatrix} = \left(p + q\frac{n_j(t)}{k_j}\right)\Delta t, \qquad \Delta t \to 0, \tag{1}$$

where $n_j(t)$ is the number of adopters connected to j at time t, k_j is the degree of node j, p describes the likelihood of j to adopt the product due to *external influences* by mass media or commercials, and q describes the likelihood of j to adopt the product due to *internal influences* (*word of mouth*) by her peers. The level of internal influences experienced by j increases linearly with the number of adopters connected to j, and is normalized by k_j, so that regardless of the network structure, the maximal internal influence that j can experience (when all his peers are adopters) is q. This normalization is justified, e.g., if individuals have a limited time to spend with their peers (or a limited attention span), so that the more peers one has, the less time/attention she has for each of them, hence the smaller their individual influences are.

To add the feature that not all members of the social network are potential adopters, we "remove" each node with probability α from the diffusion process. Thus, a "removed" node remains in the network, but remains a non-adopter at

all times. The assumption that the probability of an agent to be "removed" from the diffusion process is independent of her peer group is reasonable for e.g., diffusion of solar systems, where some residential units are physically inappropriate for installation of a solar system.

This "nodes removal" has two effects:

1. A global effect whereby the expected *market potential* decreases from M to
$$M_\alpha := (1-\alpha)M. \tag{2}$$
2. A local effect of decreasing the number of potential adopters that are connected to some nodes, namely those which are connected to "removed" nodes. Since $n_j(t) < k_j$ for those nodes, the maximal internal influence experienced by these nodes is strictly below q, see (1).

3. Complete network

We first consider the diffusion on a complete network where all M nodes are inter-connected. This case is conjectured to serve as an upper bound for all other networks with the same p and q [4]. Recall that when $\alpha = 0$, the fraction of adopters as $M \to \infty$ is [21]

$$\lim_{M\to\infty} f_{\text{complete}}(t; p, q, M, \alpha = 0) = f_{\text{Bass}}(t; p, q), \tag{3}$$

where $f_{\text{Bass}} = \frac{1-e^{-(p+q)t}}{1+(q/p)e^{-(p+q)t}}$ is the diffusion curve computed by Bass [2]. The effect of nodes "removal" from a complete network can be explicitly computed, as follows:

Lemma 1. *Consider a complete graph with M nodes, from which each node is removed from the diffusion process with probability α. Then the fraction of adopters as $M \to \infty$ is given by*

$$\lim_{M\to\infty} f_{\text{complete}}(t; p, q, M, \alpha) = (1-\alpha) f_{\text{Bass}}(t; p, q_{\alpha,\infty}), \qquad q_{\alpha,\infty} := (1-\alpha)q. \tag{4}$$

Proof. See Appendix A.

Thus, the overall effect of nodes removal on the aggregate diffusion is equivalent to reducing the market potential from M to M_α, see (2), and reducing the internal influence parameter from q to $q_{\alpha,\infty} := (1-\alpha)q$.

4. Circular networks

Next, we consider the other extreme of the "least-connected" network, where the M nodes lie on a circle, such that each node is connected to its right- and left-neighbors. This case is conjectured to serve as a lower bound for all other networks with the same p and q [4]. In the absence of nodes removal, the adoption probability (1) reads

$$\text{Prob}\begin{pmatrix} j \text{ adopts in} \\ (t, t+\Delta t)\end{pmatrix} = \left(p + q\frac{n_j(t)}{2}\right)\Delta t, \qquad \Delta t \to 0.$$

The adoption curve can be calculated explicitly, yielding [4,22]

$$\lim_{M\to\infty} f_{\text{circle}}(t; p, q, M, \alpha = 0) = 1 - e^{-(p+q)t + \frac{q}{p}(1-e^{-pt})}. \tag{5}$$

To compute the fraction of adopters under nodes removal, we use an analytic tool called the *indifference principle*. To do that, we first introduce the notion of *influential* and *noninfluential* edges:

Definition 1 (*Influential and Noninfluential Edges*)**.** Consider a directed network with M nodes (if the network in undirected, replace each undirected edge by two directed edges). Let $\Omega \subsetneqq \{1, \dots, M\}$ be a subset of the nodes, and let $\Omega^c = \{1, \dots, M\} \setminus \Omega$ be its complement. A directed edge from node s to node t is called "noninfluential to Ω" if

1. $s \in \Omega$, or
2. $s \in \Omega^c$, $t \in \Omega^c$, and there is no sequence of directed edges from t to Ω, or
3. $s \in \Omega^c$, $t \in \Omega^c$, and all sequences of directed edges from t to Ω go through the node s.

The *indifference principle* states that when calculating the probability of a set Ω of nodes at time t to consist only of non-adopters, we can add or delete noninfluential edges without affecting the adoption probability.

Lemma 2 (*Indifference Principle [22]*)**.** *Let $S_\Omega(t)$ denote the probability that all the nodes in Ω did not adopt by time t in the discrete Bass model (1). Then $S_\Omega(t)$ remains unchanged if we remove or add noninfluential edges to Ω.*

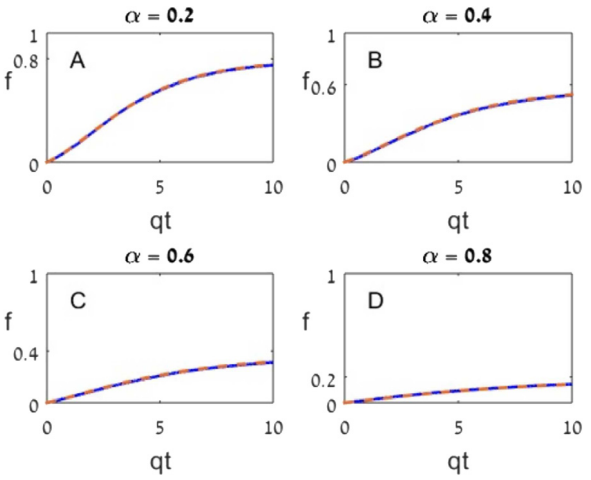

Fig. 1. Percolation on a circular network with different values of α (solid line). Dashed line is the explicit expression (6). The two lines are indistinguishable. Here $p = 0.01$, $q = 0.1$, and $M = 30{,}000$. (A) $\alpha = 0.2$. (B) $\alpha = 0.4$. (C) $\alpha = 0.6$. (D) $\alpha = 0.8$.

4.1. Explicit calculation of f_{circle}

We now apply the *indifference principle* to calculate $\lim_{M\to\infty} f_{\text{circle}}(t; p, q, M, \alpha)$.

Lemma 3. *Consider a circle with M nodes, from which each node is removed from the diffusion process with probability α. Then the fraction of adopters as $M \to \infty$ is given by*

$$\lim_{M\to\infty} f_{\text{circle}}(t; p, q, M, \alpha) = (1-\alpha)\left[1 - (1-\alpha)^2 S_\infty^{(0)}(t;\alpha) - 2\alpha(1-\alpha)S_\infty^{(1)}(t;\alpha) - \alpha^2 S_\infty^{(2)}(t)\right], \tag{6a}$$

where $S_\infty^{(2)}(t) = e^{-pt}$,

$$S_\infty^{(1)}(t;\alpha) = e^{-\left(p+\frac{q}{2}\right)t-(1-\alpha)\frac{q}{2p}\left(e^{-pt}-1\right)}\left[1 + \frac{\alpha q}{2}\int_0^t \left[e^{\left(\frac{q}{2}-p\right)\tau+(1-\alpha)\frac{q}{2p}\left(e^{-p\tau}-1\right)}\right] d\tau\right], \tag{6b}$$

and

$$S_\infty^{(0)}(t;\alpha) = e^{-(p+q)t}\left[1 + q\int_0^t \left[e^{(p+q)\tau} S_\infty^{(1)}\left(\alpha e^{-p\tau} + (1-\alpha)S_\infty^{(1)}\right)\right] d\tau\right]. \tag{6c}$$

The explicit expression (6) is indistinguishable from agent-based simulations of the discrete Bass model, see Fig. 1. It shows that f is smooth in α, but is otherwise not very informative. Hence, in Section 5 we obtain an explicit approximation for the effect of nodes removal, which is intuitive and is also valid for higher dimensions.

Proof. Let $X_j(t)$ denote the state of node j at time t, so that

$$X_j(t) = \begin{cases} 1, & \text{if } j \text{ adopted by time } t, \\ 0, & \text{otherwise,} \end{cases} \tag{7}$$

and let $\widetilde{j}$ denote the "existence" of node j, such that $\widetilde{j} =$ 'r' if j is removed from the diffusion process, and $\widetilde{j} \neq$ 'r' if j remains. Since the circular network is translation invariant and each node is removed with the same probability α, then by symmetry, $\text{Prob}\{X_j(t) = 1\}$ is independent of j. Therefore, $f_{\text{circle}}(t; p, q, M, \alpha) = \text{Prob}\{X_j(t) = 1\}$. Since $\text{Prob}\{X_j(t) = 1\} = \text{Prob}\{\widetilde{j} \neq \text{'}r\text{'}\}\text{Prob}\{X_j(t) = 1 \mid \widetilde{j} \neq \text{'}r\text{'}\}$ and $\text{Prob}\{X_j(t) = 1 \mid \widetilde{j} \neq \text{'}r\text{'}\} + \text{Prob}\{X_j(t) = 0 \mid \widetilde{j} \neq \text{'}r\text{'}\} = 1$, we have that

$$f_{\text{circle}}(t; p, q, M, \alpha) = (1-\alpha)(1 - \text{Prob}\{X_j(t) = 0 \mid \widetilde{j} \neq \text{'}r\text{'}\}). \tag{8}$$

By (8) and by the law of total probability, we get

$$f_{\text{circle}}(t; p, q, M, \alpha) = (1-\alpha)\left(1 - (1-\alpha)^2 S^{(0)}(t; M, \alpha) - 2\alpha(1-\alpha)S^{(1)}(t; M, \alpha) - \alpha^2 S^{(2)}(t; M, \alpha)\right),$$

where $\{S^{(k)}(t; M, \alpha)\}_{k=0}^2$ are the probabilities of node j to remain a non-adopter by time t in a circular network with M nodes, provided that k of his neighbors are removed.

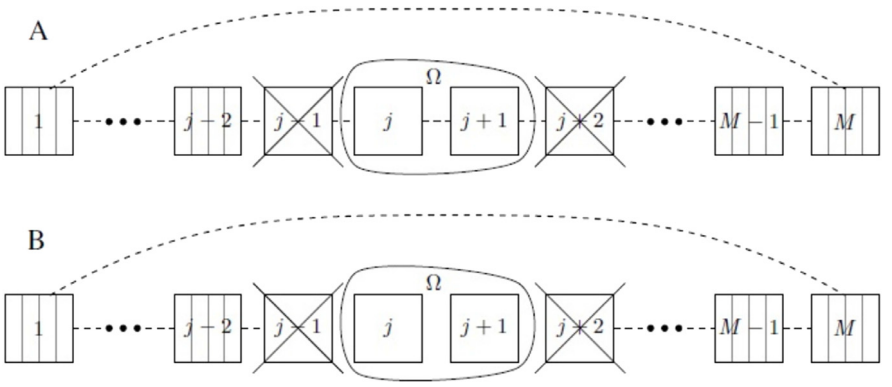

Fig. 2. Equivalent networks for the calculation of $\text{Prob}\{X_j(t) = 0, X_{j+1}(t) = 0 \mid \widetilde{j-1} = \text{`r'}, \widetilde{j} = \widetilde{j+1} \neq \text{`r'}, \widetilde{j+2} = \text{`r'}\}$. Solid and dashed lines correspond to "influential" and "noninfluential" edges to $\Omega = \{j, j+1\}$, respectively. We denote by ⊠, ▥, and □ a node which is removed, removed with probability α, and not removed, respectively. (A) Circular one-dimensional network, under the assumption that $\widetilde{j-1} = \text{`r'}$, $\widetilde{j} = \widetilde{j+1} \neq \text{`r'}$, $\widetilde{j+2} = \text{`r'}$. The links that emanate from the removed nodes are noninfluential to Ω. (B) The noninfluential links from $j-1$ to j, from j to $j+1$, and from $j+1$ to $j+2$ are deleted.

When both neighbors of j are removed, its evolution equation is given by $\frac{\text{d}}{\text{dt}}S^{(2)}(t; M, \alpha) = -pS^{(2)}(t; M, \alpha)$, see e.g. Fibich et al. [22, eq. (3.8)], subject to the initial condition $S^{(2)}(0; M, \alpha) = 1$. Therefore, $S^{(2)}(t; M, \alpha) = e^{-pt}$ for all M, and so

$$S^{(2)}_{\infty}(t; \alpha) := \lim_{M\to\infty} S^{(2)}(t; M, \alpha) = e^{-pt}. \tag{9}$$

To derive the evolution equation for $S^{(1)}(t; M, \alpha)$, we assume, without loss of generality, that $\widetilde{j-1} = \text{`r'}$, and $\widetilde{j} = \widetilde{j+1} \neq \text{`r'}$. Following Fibich and Gibori [4, proof of Lemma 8], the evolution equation for $S^{(1)}(t; M, \alpha)$ is given by

$$\frac{\text{d}}{\text{dt}}S^{(1)}(t; M, \alpha) + \left(p + \frac{q}{2}\right) S^{(1)}(t; M, \alpha) = \frac{q}{2}\text{Prob}\{X_j(t) = 0, X_{j+1}(t) = 0 \mid \widetilde{j-1} = \text{`r'}, \widetilde{j} = \widetilde{j+1} \neq \text{`r'}\}.$$

Using the conditional probabilities on the removal of node $j+2$ gives

$$\begin{aligned}\frac{\text{d}}{\text{dt}}S^{(1)}(t; M, \alpha) + \left(p + \frac{q}{2}\right) S^{(1)}(t; M, \alpha) = \\ \alpha\frac{q}{2}\text{Prob}\{X_j(t) = 0, X_{j+1}(t) = 0 \mid \widetilde{j-1} = \text{`r'}, \widetilde{j} = \widetilde{j+1} \neq \text{`r'}, \widetilde{j+2} = \text{`r'}\} \\ + (1-\alpha)\frac{q}{2}\text{Prob}\{X_j(t) = 0, X_{j+1}(t) = 0 \mid \widetilde{j-1} = \text{`r'}, \widetilde{j} = \widetilde{j+1} = \widetilde{j+2} \neq \text{`r'}\}.\end{aligned} \tag{10}$$

By the *indifference principle* (Lemma 2) we can calculate the probability

$$\text{Prob}\{X_j(t) = 0, X_{j+1}(t) = 0 \mid \widetilde{j-1} = \text{`r'}, \widetilde{j} = \widetilde{j+1} \neq \text{`r'}, \widetilde{j+2} = \text{`r'}\}$$

from the equivalent network in Fig. 2B. Therefore, by (9),

$$\text{Prob}\{X_j(t) = 0, X_{j+1}(t) = 0 \mid \widetilde{j-1} = \text{`r'}, \widetilde{j} = \widetilde{j+1} \neq \text{`r'}, \widetilde{j+2} = \text{`r'}\} = \left(S^{(2)}(t; M, \alpha)\right)^2 = e^{-2pt}. \tag{11}$$

Similarly, we can use the *indifference principle* to calculate the probability

$$\text{Prob}\{X_j(t) = 0, X_{j+1}(t) = 0 \mid \widetilde{j-1} = \text{`r'}, \widetilde{j} = \widetilde{j+1} = \widetilde{j+2} \neq \text{`r'}\}$$

from the equivalent network in Fig. 3B. Therefore,

$$\text{Prob}\{X_j(t) = 0, X_{j+1}(t) = 0 \mid \widetilde{j-1} = \text{`r'}, \widetilde{j} = \widetilde{j+1} = \widetilde{j+2} \neq \text{`r'}\} = e^{-pt}S^{(1)}(t; M-1, \alpha). \tag{12}$$

Plugging (11) and (12) into (10), and taking the limit $M \to \infty$, yield the following ODE for $S^{(1)}_{\infty} := \lim_{M\to\infty} S^{(1)}(t; M, \alpha)$:

$$\frac{\text{d}}{\text{dt}}S^{(1)}_{\infty}(t; \alpha) + \left(p + \frac{q}{2} - \frac{q}{2}(1-\alpha)e^{-pt}\right) S^{(1)}_{\infty}(t; \alpha) = \frac{q}{2}\alpha e^{-2pt}, \tag{13}$$

subject to the initial condition $S^{(1)}_{\infty}(0; \alpha) = 1$. The solution of (13) is given by (6b). The derivation of (6c) is similar, see Appendix C.

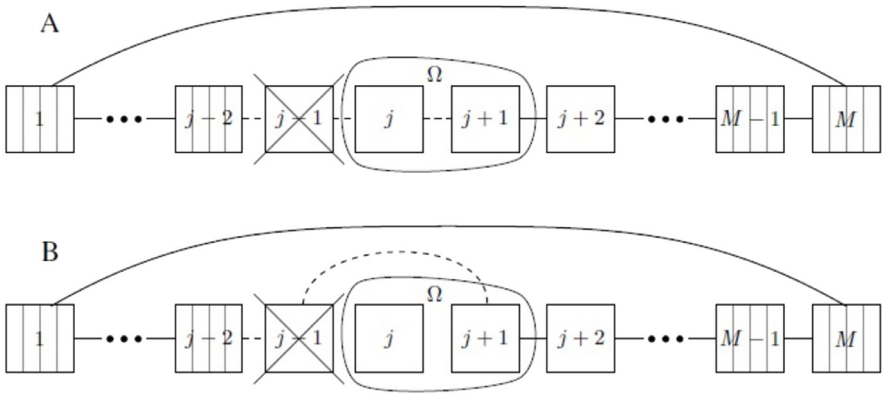

Fig. 3. Equivalent networks for the calculation of $\text{Prob}\{X_j(t) = 0, X_{j+1}(t) = 0 \mid \widetilde{j-1} = \text{'r'}, \widetilde{j} = \widetilde{j+1} = \widetilde{j+2} \neq \text{'r'}\}$. (A) Circular one-dimensional network, under the assumption that $\widetilde{j-1} = \text{'r'}$, $\widetilde{j} = \widetilde{j+1} = \widetilde{j+2} \neq \text{'r'}$. (B) The noninfluential links from $j-1$ to j, and from j to $j+1$ are deleted. Instead, a noninfluential link that connects nodes $j-1$ and $j+1$ is added.

5. *D*-dimensional Cartesian networks

Next, we consider the percolation on D-dimensional Cartesian grids, where each node is connected to its $2D$ nearest neighbors. The two-dimensional case is relevant for products that spread predominantly through internal influences by geographical neighbors, such as residential rooftop solar systems [9,10]. In the absence of node removal, the adoption probability (1) reads

$$\text{Prob}\left(\begin{matrix}j \text{ adopts in}\\(t, t+\Delta t)\end{matrix}\right) = \left(p + q\frac{n_j(t)}{2D}\right)\Delta t, \qquad \Delta t \to 0.$$

There are no explicit expressions such as (5) or (6) for $f(t)$ on Cartesian grids with $D > 1$, without or with percolation, respectively. We can, however, approximate the effect of the percolation parameter α on the aggregate adoption:

Lemma 4. *Consider a D-dimensional Cartesian networks with M nodes, from which each node is removed from the diffusion process with probability α. As $M \to \infty$, the adoption curve depends on the percolation parameter α via the relation*

$$\lim_{M\to\infty} f_D(t; p, q, M, \alpha) \sim (1-\alpha) \lim_{M\to\infty} f_D(t; p, q_{\alpha,D}, M, \alpha = 0), \qquad q_{\alpha,D} := (1-\alpha)^{1+1/D} q. \tag{14}$$

Proof. We provide an informal proof in Section 5.1.

Remark 1. The case of a complete network corresponds to $D \to \infty$. Indeed, as $D \to \infty$, relation (14) reduces to (4).

Approximation (14) is in excellent agreement with the agent-based simulations for $0.2 \le \alpha \le 0.8$ and $D = 1, 2, 3$, see Figs. 4–6, respectively. Lemma 4 shows that the complex effect of random node removal on the aggregate diffusion is equivalent to the following two simple effects:

1. Reducing the market potential from M to M_α, see (2).
2. Reducing the internal influences parameter from q to $q_{\alpha,D} := (1-\alpha)^{1+1/D} q$.

In particular, percolation is qualitatively similar to diffusion, and its dependence on α is smooth.

5.1. Informal Proof of Lemma 4

Following [4], we visualize the diffusion process in the discrete Bass model as an ongoing random creation of external adopters ("*seeds*"). Once created, each seed expands through internal adoptions into a cluster of adopters, and expanding clusters can merge into larger clusters. In addition, on D-dimensional Cartesian grids, clusters expand, on average, as D-dimensional circles/balls, whose radii increases linearly with time, i.e.,

$$R_k(t) \approx c_D\, q(t - t_k), \tag{15}$$

where R_k and t_k are the radius and creation time of the kth cluster, respectively, and c_D is a constant that only depends on the dimension.

Fig. 7 shows a typical expansion of a cluster in a two-dimensional Cartesian network, from which we removed each node with probability α. Here we placed a single external adopter (seed) at the center at $t = 0$, and all subsequent

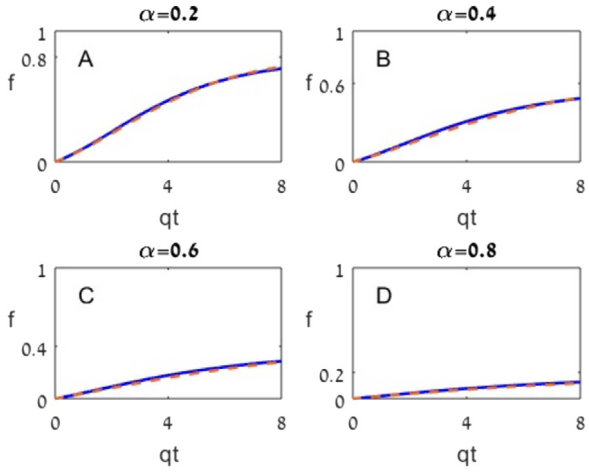

Fig. 4. Percolation on a 1D grid, as a function of time (solid line). The dashed line is the asymptotic approximation (14). The two lines are nearly indistinguishable. Here $p = 0.01$, $q = 0.1$ and $M = 10{,}000$. (A) $\alpha = 0.2$. (B) $\alpha = 0.4$. (C) $\alpha = 0.6$. (D) $\alpha = 0.8$.

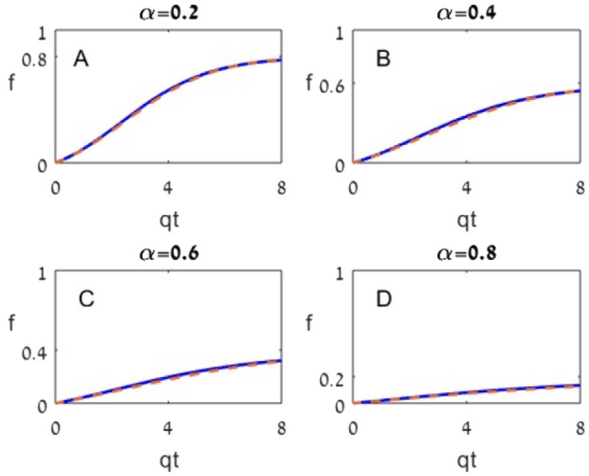

Fig. 5. Same as Fig. 4 with $D = 2$.

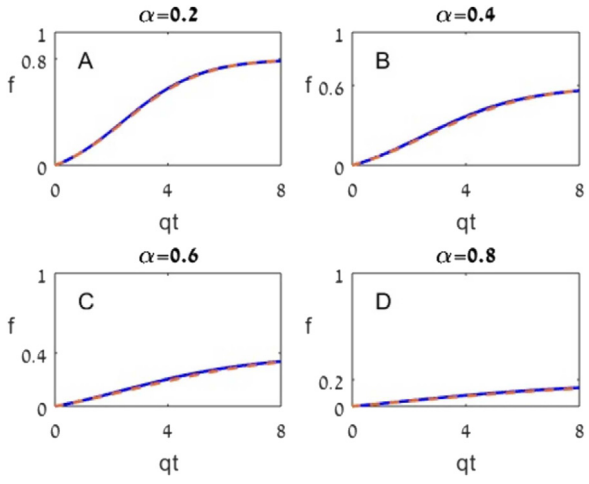

Fig. 6. Same as Fig. 4 with $D = 3$.

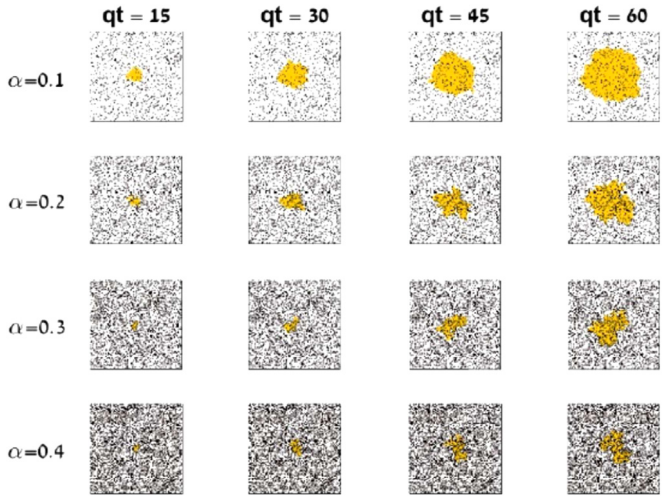

Fig. 7. Typical evolution of a single cluster in a two-dimensional Cartesian grid, from which each node is removed with probability α. Here black, white, and yellow pixels correspond to removed nodes, non-adopters, and adopters, respectively.

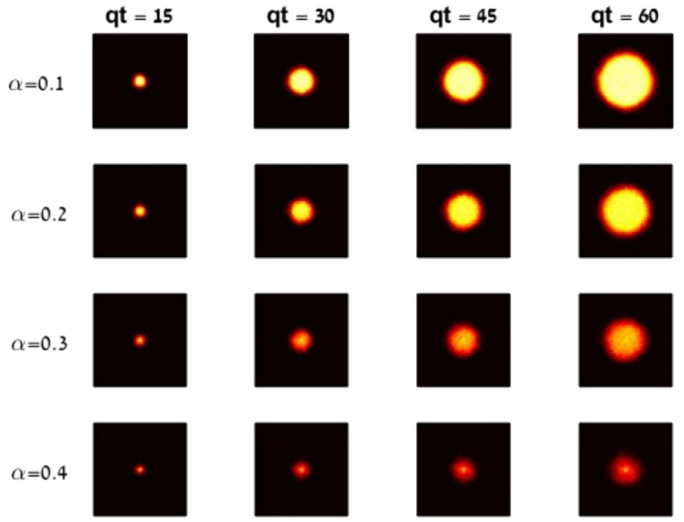

Fig. 8. Same as Fig. 7, but averaged over 100 simulations. Here, white corresponds to 100% adoption and black to 0% adoption. Removed nodes are counted as non-adopting.

adoptions were purely internal (i.e., are according to (1) with $p = 0$ and $k_j = 4$). For sufficiently small α, the cluster continues to expand as a circle. As α increases, the cluster shape becomes less regular. Once averaged over many clusters, however, the average cluster shape remains circular even as α increases, see Fig. 8.

For a given cluster volume with radius R, only $(1-\alpha)$ of its nodes are adopters (the rest are removed nodes). Therefore, its outward expansion rate due to its boundary adopters is equivalent to that of a cluster with no removed nodes and a radius of $(1-\alpha)^{1/D}R$. In addition, only $1-\alpha$ of the non-cluster nodes which are connected to the boundary adopters are potential adopters. Therefore, the cluster expansion rate reduces by a factor of $(1-\alpha)^{1+1/D}$, i.e., $R_k(t;\alpha) \approx c_D(1-\alpha)^{1+1/D}q(t-t_k)$. In other words, the cluster expansion is given by (15) with q replaced by $q_{\alpha,D} := (1-\alpha)^{1+1/D}q$. For a given cluster volume, however, only $1-\alpha$ of its nodes are adopters. Hence, the result follows.

5.2. Breakdown of approximation (14)

Approximation (14) is based on the assumption that under nodes removal, clusters still grow on average as D-dimensional balls, albeit at the reduced constant expansion rate $q_{\alpha,D}$. Since externals seeds are created at the rate of p, the maximal diameter of an isolated cluster is roughly $\frac{q_{\alpha,D}}{p}$ (once it gets larger, the cluster merges with other clusters). In addition, when α exceeds some dimension-dependent threshold $\alpha_c = \alpha_c(D)$, the network breaks into disconnected

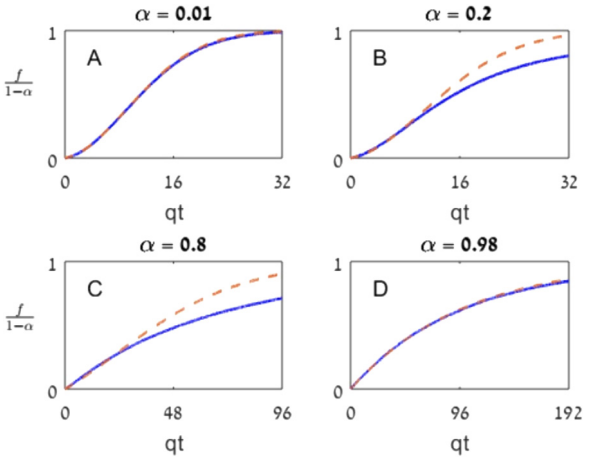

Fig. 9. Same as Fig. 4 with $q/p = 100$. Here the y axis is $f/(1-\alpha)$. (A) $\alpha = 0.01$. (B) $\alpha = 0.2$. (C) $\alpha = 0.8$. (D) $\alpha = 0.98$.

components (see Section 9.1). As α further increases above α_c, the size of these disconnected components decreases. Once their diameter gets below $\frac{q_{\alpha,D}}{p}$, the isolated clusters cannot grow as assumed, and so approximation (14) breaks down. As α further increases and approaches 1, however, approximation (14) becomes valid again, since the few remaining nodes are isolated from each other and so they can only adopt due to external effects, which is consistent with $q_{\alpha,D} \to 0$ as $\alpha \to 1$ in (14).

In the one-dimensional case $\frac{q_{\alpha,D}}{p} = \frac{(1-\alpha)^2 q}{p}$ and $\alpha_c = 0$ (i.e., the network breaks into isolated intervals for any $\alpha > 0$). The lengths of these intervals is geometrically distributed with parameter α, and so the average interval length is $\frac{1}{\alpha}$. Therefore, approximation (14) breaks down when $\frac{(1-\alpha)^2 q}{p} \gg \frac{1}{\alpha}$, i.e., when

$$C_{1D}(\alpha, q, p) := (1-\alpha)^2 \alpha \frac{q}{p} \gg 1. \tag{16}$$

To confirm condition (16) numerically, we computed the percolation dynamics for $D = 1$ and $q/p = 100$. When $\alpha = 0.01$, condition (16) is not satisfied ($C_{1D} = 0.98$), and approximation (14) indeed holds (Fig. 9A). For $\alpha = 0.2$ and $\alpha = 0.8$ condition (16) is satisfied ($C_{1D} = 12.8$ and $C_{1D} = 3.2$, respectively), and approximation (14) indeed breaks down (Fig. 9B and C, respectively). Finally, as α further increases and becomes close to one ($\alpha = 0.98$), condition (16) is again not satisfied ($C_{1D} = 0.04$) and approximation (14) indeed holds again (Fig. 9D).

Condition (16) also explains why for $D = 1$ and $q/p = 10$, approximation (14) holds for any α, see Fig. 4. Indeed, since $(1-\alpha)^2\alpha \le \frac{4}{27}$ for $0 \le \alpha \le 1$, then $C_{1D} \le \frac{40}{27} \approx 1.5$.

The situation is similar in higher dimensions. For example, on a two-dimensional square lattice $\alpha_c \approx 0.41$. Hence, approximation (14) is valid for α below α_c (Fig. 10A), starts to break down for α slightly above α_c (Fig. 10b), breaks down more dramatically as α further increases (Fig. 10C), but improves again as α approaches one (Fig. 10D).

6. Small-world networks

Watts and Strogatz [23] suggested that social networks have a small-world structure, whereby most connections are local, but there are also some random long-range connections (see e.g. Fig. 11A). They showed that even a small fraction of long-range connections can lead to a dramatic reduction in the average distance between nodes. As a result, epidemics spread much faster on networks with a small-world structure.

In Fig. 11B we numerically compute the fraction of adopters in percolation on a circle from which each node is removed from the diffusion process with probability $\alpha = 0.2$. We then add 5% random long-range links and repeat this simulation. The small-world structure has a negligible effect on the diffusion, which is consistent with previous studies [4,20]. Briefly, this is because a small-world structure affects global properties of the network, whereas diffusion in the Bass model depends on local properties of the network. See Section 9 for further discussion.

Since the addition of random long-range links has a negligible effect on the diffusion, we can approximate the adoption curve for this case with (14). This approximation can be somewhat improved if one uses (14) with an "effective" external parameter $p + 0.05qf/3$ instead of p, see Fig. 11C. This is because the long-range connections can be considered to be a sort-of "external source". Each node gets, on average, 0.05 additional connections. Since most nodes get only 1 long-range connection in addition to its 2 regular connections, and the weights of all the links sum up to q, the weights of the long-range connections are $q/3$. Furthermore, these long-range connections originate from other nodes of the network, and so these connections are "active" with probability f.

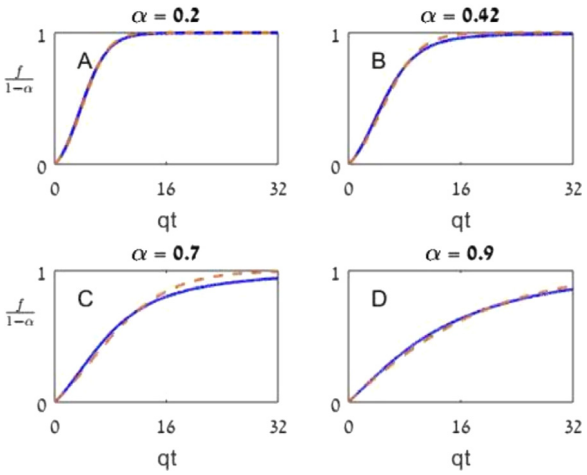

Fig. 10. Same as Fig. 9 with $D = 2$ and $q/p = 20$. (A) $\alpha = 0.2$. (B) $\alpha = 0.42$. (C) $\alpha = 0.7$. (D) $\alpha = 0.9$.

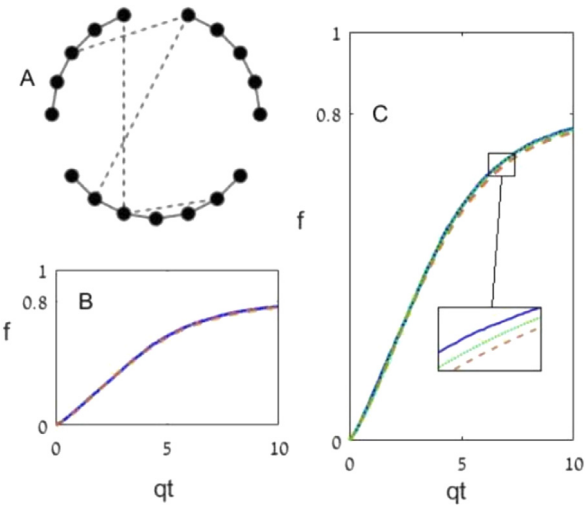

Fig. 11. (A) A circle from which each node is removed with probability $\alpha = 0.2$, with the addition of 5% long-range random links (dashes). (B) Percolation on a circle from which each node is removed with probability $\alpha = 0.2$, with (solid) and without (dashes) the addition of 5% long-range random links. The two lines are nearly indistinguishable. Here $p = 0.01$, $q = 0.1$, and $M = 10{,}000$. (C) The solid line is the same as in B. The dashed and the dotted lines are the analytical approximation (14) with external parameter p and $p + 0.05qf/3$, respectively.

7. Scale-free networks

Many social networks are believed to be scale-free [17]. We constructed scale-free networks using the Barabási–Albert (BA) preferential-attachment algorithm [24], in which each new node makes m new links with the existing network nodes, such that the probability of a new node to connect to node i_0 is $k_{i_0}/\sum_i k_i$, where k_i is the degree of node i. By (1), the marginal effect of each adopter connected to j is q/k_j.

Previously [20], it was observed numerically that the aggregate diffusion on a BA scale-free network with parameter m is nearly identical to that on a Cartesian network with $D = m$, i.e.,

$$f_D(t; p, q, \alpha = 0) \sim f^{\text{scale-free}}_{m=D}(t; p, q, \alpha = 0). \tag{17}$$

For example, diffusion on a scale-free network with $m = 2$ is nearly identical to that on a 2D Cartesian network (Fig. 12). This result is very surprising, since apart from having the same average degree of $\langle k_i \rangle = 2m = 2D$, the degree distributions of Cartesian and scale-free networks are as far apart as they can be: the fraction of nodes of degree k are [25]

$$p_k^{\text{Cartesian}} = \begin{cases} 1, & k = 2D, \\ 0, & k \neq 2D, \end{cases} \qquad p_k^{\text{scale-free}} = \begin{cases} 0, & k < m, \\ \frac{2m(m+1)}{k(k+1)(k+2)}, & k \geq m, \end{cases}$$

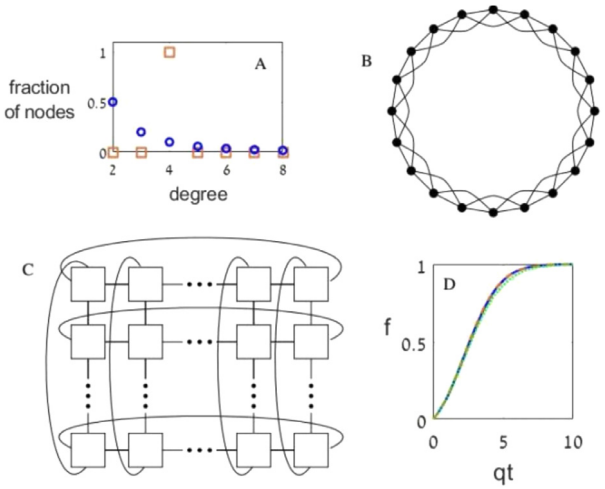

Fig. 12. (A) Degree distributions of a scale-free network with $m = 2$ (○) and a 2D network (□). (B) 1D network in which each node is connected to two neighbors on each side. (C) 2D network with nearest neighbor connections. (D) Diffusion on a scale-free network with $m = 2$ (solid), on the two-dimensional Cartesian network (dashes), and on the one-dimensional network (dots). All three networks have the same average degree $\langle k_i \rangle = 4$. Here $p = 0.01$, $q = 0.1$, and $M = 30{,}000$.

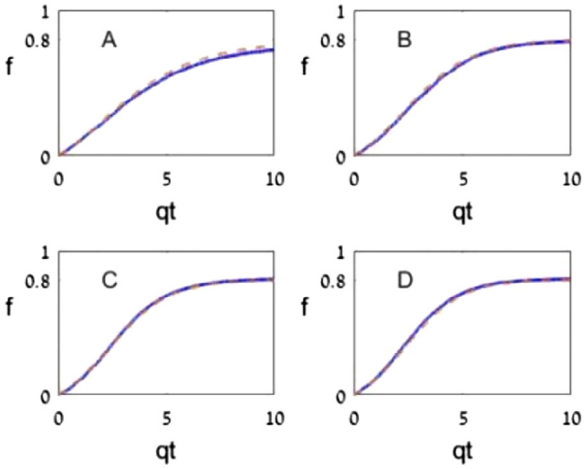

Fig. 13. Percolation on scale-free (solid) and Cartesian (dashes) networks with $p = 0.01$, $q = 0.1$, and $\alpha = 0.2$. The two lines are nearly indistinguishable. (A) $m = D = 1$. (B) $m = D = 2$. (C) $m = D = 3$. (D) $m = D = 4$.

see Fig. 12A. Of course, one possible explanation could be that diffusion only depends on the average degree. This explanation, however, is wrong. For example, the diffusion on a 1D circular network in which each node is connected to two neighbors on each side (Fig. 12B) is slower than on a 2D network with nearest neighbors connections (Fig. 12C), even though this network has the same average degree as the previous two networks, see Fig. 12D. Thus, the equivalence (17) of diffusion on Cartesian and scale-free networks is more delicate, and is currently not well understood.

Fig. 13 shows that the surprising equivalence (17) between Cartesian and scale-free networks persists when we remove each node with probability α, i.e.,

$$f_D(t; p, q, \alpha) \sim f_{m=D}^{\text{scale-free}}(t; p, q, \alpha).$$

Therefore, by relation (14), $f_m^{\text{scale-free}}(t; p, q, \alpha)$ depends on α via the asymptotic relation

$$f_m^{\text{scale-free}}(t; p, q, \alpha) \sim (1-\alpha) f_m^{\text{scale-free}}(t; p, q_{\alpha,m}, \alpha = 0), \qquad q_{\alpha,m} := (1-\alpha)^{1+\frac{1}{m}} q, \tag{18}$$

as is confirmed numerically in Fig. 14.

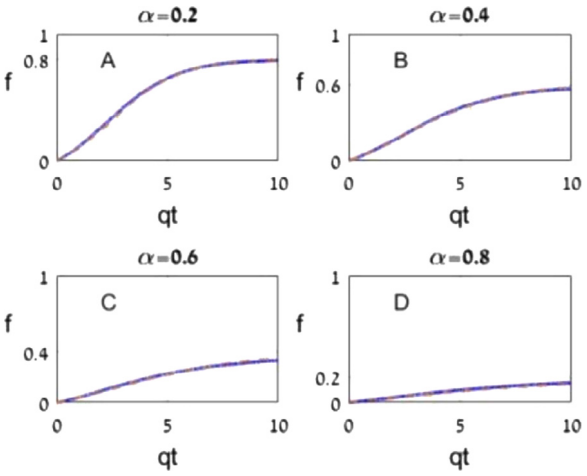

Fig. 14. Same as Fig. 4 on a scale-free network with $m = 2$ and $M = 20{,}000$. The dashed line is the asymptotic approximation (18). The two lines are nearly indistinguishable.

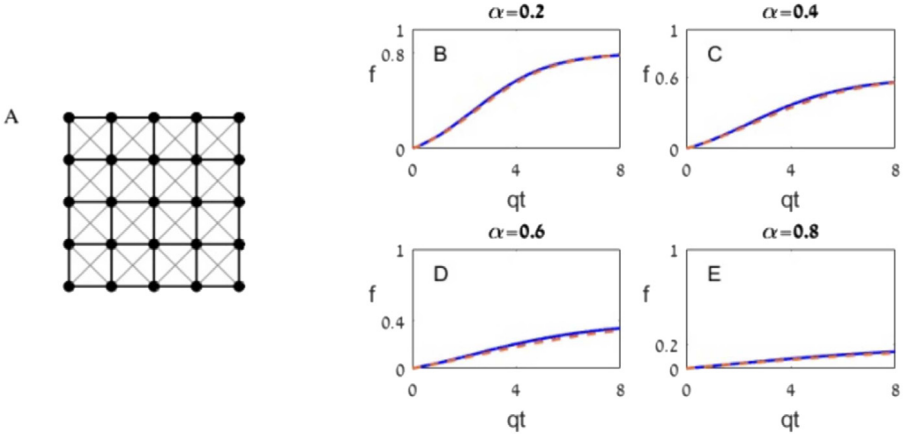

Fig. 15. (A) 2D Cartesian network with "long-range" diagonal connections (gray). (B)–(E) Same as Fig. 4, when each node is connected to its eight nearest nodes. Here $p = 0.01$, $q_1 = 0.07$ and $q_2 = 0.03$. The dashed line is the analytic prediction (19). The two lines are nearly indistinguishable.

8. Beyond nearest-neighbor effects

In diffusion of residential rooftop solar systems, the peers effect of the neighbors who already installed a solar system on potential adopters decreases with distance, but extends well beyond the next-door neighbor [10]. To allow for such "long-range" influences, we consider a 2D Cartesian network in which node (i, j) is influenced with weight $q_1/4$ by its four nearest nodes $(i, j \pm 1)$ and $(i \pm 1, j)$, and with weight $q_2/4$ by its "further-away" four diagonal nodes $(i \pm 1, j \pm 1)$, see Fig. 15A. To conform with (1), we impose $q_1 + q_2 = q$. Motivated by (14), we test in Fig. 15B whether

$$f(t; p, q_1, q_2, \alpha) \approx (1-\alpha) f(t; p, q_{1,\alpha}, q_{2,\alpha}, \alpha = 0), \qquad q_{i,\alpha} := (1-\alpha)^{3/2} q_i. \tag{19}$$

The agreement is quite impressive, though not as good as in Fig. 5. This is because the "long-range" diagonal connections enable the cluster to expand (see Section 5.1) while "leaving behind" isolated regions of potential adopters. The potential adopters in these regions eventually adopt as well, but the effect of percolation on this "secondary filling process" is not given by $q_{i,\alpha} := (1-\alpha)^{3/2} q_i$.

9. Discussion

The main outcome of this study is that at the aggregate level, percolation of new products is qualitatively similar to the case where everyone in the market is a potential adopter. Specifically, as the fraction α of "removed" nodes increases, the market potential decreases by $(1-\alpha)$, the external influence parameter p remains unchanged, and the internal influence parameter q decreases by $(1-\alpha)^k$, where $k = 1$ for a complete network, $k = 1 + 1/D$ for D-dimensional Cartesian networks, and $k = 1 + 1/m$ for scale-free networks with parameter m.

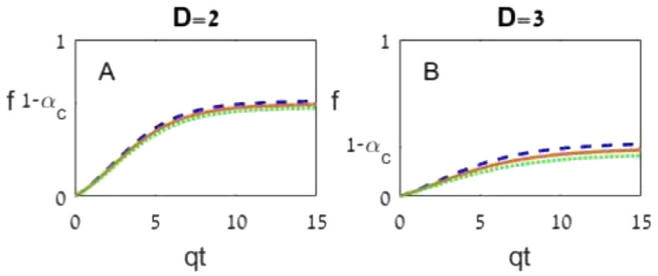

Fig. 16. Percolation on a D-dimensional Cartesian grid with $M = 10{,}000$ nodes, as a function of time. Here $p = 0.01$, $q = 0.1$, and $0.95\alpha_c$ (dashes), α_c (solid) and $1.05\alpha_c$ (dots), where α_c is the threshold for the existence of a giant component. (A) $D = 2$, $\alpha_c \approx 1-0.593$. (B) $D = 3$, $\alpha_c \approx 1-0.3116$.

9.1. Absence of a phase transition

A key property of percolation models is the occurrence of a phase transition at a certain critical threshold [e.g.,17,26,27]. For example, the percolation threshold for the existence of a *giant component* (i.e., a connected component of nodes that contains a positive fraction of the network nodes) is $\alpha_c = 0$ on a one-dimensional network, $\alpha_c \approx 1 - 0.593 \approx 0.4$ on a two-dimensional square lattice, and $\alpha_c \approx 1 - 0.3116 \approx 0.7$ on a three-dimensional cubic lattice. In this study we showed, however, that the diffusion curves are smooth in α. Therefore, there is no phase transition in percolation of new products. For example, Fig. 16 shows numerically that on two-dimensional and three-dimensional grids, there are only minor changes in the adoption curve as α varies between $0.95\alpha_c$ and $1.05\alpha_c$.

Briefly, a phase transition occurs at α_c when the diffusion depends on the network connectivity. This is the case, for example, in Susceptible–Infected (SI) models of epidemics [17], where the disease starts from several "infected" nodes ("patients zero") that exist at $t = 0$, and all subsequent infections are purely internal ($p = 0$), since then for the epidemics to spread out, at least one "patient zero" should belong to the giant component. Hence, in SI models the size of the giant component determines the extent to which the epidemics would spread out. Diffusion of new products, however, starts from numerous "seeds" (external adopters) which are continuously generated in time, see (1), and then expand into clusters through internal adoptions. Since the diffusion in each connected sub-network is independent, the issue of global connectivity has a minor influence on the diffusion. Nodes removal can also change the sub-network topology. This change is gradual, however, and is therefore continuous in α.

The above discussion explains the apparent disagreement between our results and those of previous studies on percolation of new products [11–16], which reported on a threshold above which the product did not diffuse to its entire market potential. Indeed, in those studies the diffusion started from one or several initial consumers, and all subsequent adoptions where purely internal (i.e., as in the SI model). In this study, however, we used the discrete Bass model (1) in which external adopters are continuously generated in time, which we believe is more appropriate for new products.

Declaration of competing interest

The authors declare that they have no known competing financial interests or personal relationships that could have appeared to influence the work reported in this paper.

Acknowledgments

We thank K. Gillingham and O. Yakir for useful discussions. This material is based upon work supported by the Department of Energy under Award Numbers DE-EE0007657.

Appendix A. Proof of Lemma 1.

When we remove j nodes from the diffusion process, where $j = 0, \ldots, M$, we effectively obtain a complete sub-graph of size M_j, internal influence $p_j^M = p$, and external influence q_j^M, where

$$M_j = M - j, \qquad q_j^M = q\left(1 - \frac{j}{M-1}\right). \tag{A.1}$$

Since each node is removed with probability α, the expected fractional diffusion is

$$f_{\text{complete}}(t; p, q, M, \alpha) = \sum_{j=0}^{M} \binom{M}{j} \alpha^j (1-\alpha)^{M-j} \frac{M_j}{M} f_{\text{complete}}(t; p, q_j^M, M_j, \alpha = 0).$$

Let $0 < \epsilon \ll 1$. Then

$$f_{\text{complete}}(t; p, q, M, \alpha) = I_1 + I_2, \tag{A.2}$$

where

$$I_1 := \sum_{\substack{\epsilon < |\frac{j}{\alpha M} - 1| \\ 0 \le j \le M}} \binom{M}{j} \alpha^j (1-\alpha)^{M-j} \frac{M_j}{M} f_{\text{complete}}(t; p, q_j^M, M_j, \alpha = 0),$$

$$\begin{aligned} I_2 :&= \sum_{|\frac{j}{\alpha M} - 1| \le \epsilon} \binom{M}{j} \alpha^j (1-\alpha)^{M-j} \frac{M_j}{M} f_{\text{complete}}(t; p, q_j^M, M_j, \alpha = 0) \\ &= \sum_{j=J_1(\epsilon)}^{J_2(\epsilon)} \binom{M}{j} \alpha^j (1-\alpha)^{M-j} \frac{M_j}{M} f_{\text{complete}}(t; p, q_j^M, M_j, \alpha = 0), \end{aligned}$$

and

$$J_1(\epsilon) = \lceil \alpha M(1-\epsilon) \rceil, \qquad J_2(\epsilon) = \lfloor \alpha M(1+\epsilon) \rfloor. \tag{A.3}$$

Since all the summands of I_1 are positive and smaller than one,

$$0 \le I_1 \le \sum_{\substack{\epsilon < |\frac{j}{\alpha M} - 1| \\ 0 \le j \le M}} \binom{M}{j} \alpha^j (1-\alpha)^{M-j} \le 2e^{-\alpha M \epsilon^2/3}, \tag{A.4}$$

where in the last inequality we used the Chernoff bound [28]. To bound I_2 we use the *dominance principle* Appendix B, to conclude that as the number of removed nodes increases, the expected number of adopters decreases. Hence, the series $\left\{M_j f_{\text{complete}}(t; p, q_j^M, M_j, \alpha = 0)\right\}_{j=0}^M$ is monotonically decreasing in j. Extracting a constant term from the sum and using Chernoff bound again yields

$$\begin{aligned} I_2 &\ge \frac{M_{J_2}}{M} f_{\text{complete}}(t; p, q_{J_2}^M, M_{J_2}, \alpha = 0) \sum_{j=J_1(\epsilon)}^{J_2(\epsilon)} \binom{M}{j} \alpha^j (1-\alpha)^{M-j} \\ &\ge \frac{M_{J_2}}{M} f_{\text{complete}}(t; p, q_{J_2}^M, M_{J_2}, \alpha = 0) \left(1 - 2e^{-\alpha M \epsilon^2/3}\right). \end{aligned} \tag{A.5a}$$

Similarly, using $\sum_{j=0}^M \binom{M}{j} \alpha^j (1-\alpha)^{M-j} = 1$, one obtains

$$I_2 \le \frac{M_{J_1}}{M} f_{\text{complete}}(t; p, q_{J_1}^M, M_{J_1}, \alpha = 0) \sum_{j=J_1(\epsilon)}^{J_2(\epsilon)} \binom{M}{j} \alpha^j (1-\alpha)^{M-j} \le \frac{M_{J_1}}{M} f_{\text{complete}}(t; p, q_{J_1}^M, M_{J_1}, \alpha = 0). \tag{A.5b}$$

By (A.2), (A.4), and (A.5),

$$\begin{aligned} \frac{M_{J_2}}{M} f_{\text{complete}}(t; p, q_{J_2}^M, M_{J_2}, \alpha = 0) \left(1 - 2e^{-\alpha M \epsilon^2/3}\right) \le f_{\text{complete}}(t; p, q, M, \alpha) \le \\ 2e^{-\alpha M \epsilon^2/3} + \frac{M_{J_1}}{M} f_{\text{complete}}(t; p, q_{J_1}^M, M_{J_1}, \alpha = 0). \end{aligned} \tag{A.6}$$

By (A.1) and (A.3), for M sufficiently large,

$$\widetilde{q_+}(\epsilon) := (1 - \alpha(1-2\epsilon))q \ge q_{J_1}^M, \qquad \widetilde{q_-}(\epsilon) := (1 - \alpha(1+2\epsilon))\, q \le q_{J_2}^M. \tag{A.7}$$

By repeated use of the *dominance principle* (Appendix B), $f_{\text{complete}}(t; p, q, M, \alpha = 0)$ is monotonically increasing in q. Hence, (A.6) and (A.7) give

$$\begin{aligned} \frac{M_{J_1}}{M} f_{\text{complete}}(t; p, \widetilde{q_-}(\epsilon), M_{J_1}, \alpha = 0) \left(1 - 2e^{-\alpha M \epsilon^2/3}\right) \le f_{\text{complete}}(t; p, q, M, \alpha) \le \\ 2e^{-\alpha M \epsilon^2/3} + \frac{M_{J_2}}{M} f_{\text{complete}}(t; p, \widetilde{q_+}(\epsilon), M_{J_2}, \alpha = 0). \end{aligned} \tag{A.8}$$

By (A.1) and (A.3),

$$\begin{aligned} &\lim_{M\to\infty} \frac{M_{J_1}}{M} = 1 - \alpha(1-\epsilon), \qquad \lim_{M\to\infty} \frac{M_{J_2}}{M} = 1 - \alpha(1+\epsilon), \\ &\lim_{M\to\infty} M_{J_1} = \lim_{M\to\infty} M_{J_2} = \infty, \qquad \lim_{M\to\infty} 2e^{-\alpha M \epsilon^2/3} = 0. \end{aligned} \tag{A.9}$$

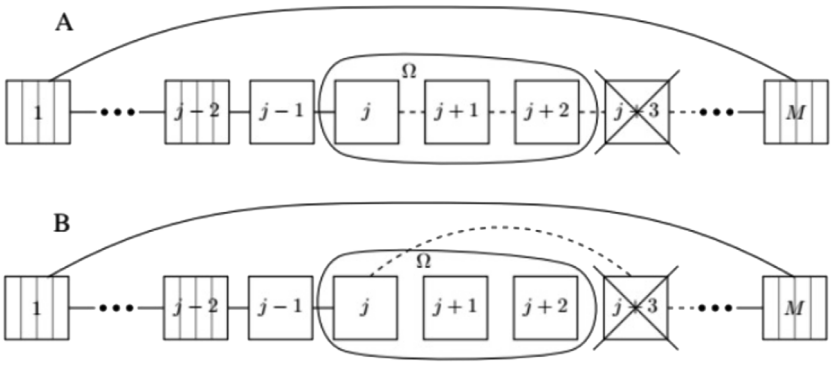

Fig. C.17. Equivalent networks for the calculation of $\text{Prob}\{X_j(t)=0, X_{j+1}(t)=0, X_{j+2}(t)=0 \mid \widetilde{j-1}=\widetilde{j}=\widetilde{j+1}=\widetilde{j+2}\neq \text{'r'},\ \widetilde{j+3}=\text{'r'}\}$. Here $\Omega=\{j, j+1, j+2\}$. (A) Circular one-dimensional network, under the assumption that $\widetilde{j-1}=\widetilde{j}=\widetilde{j+1}=\widetilde{j+2}\neq$ 'r', $\widetilde{j+3}=$ 'r'. (B) The noninfluential links from j to $j+1$, from $j+1$ to $j+2$, and from $j+2$ to $j+3$ are deleted. Instead, a noninfluential link that connects nodes j and $j+3$ is added.

Hence, combining (3), (A.8) and (A.9) gives

$$(1-\alpha(1+\epsilon))f_{\text{Bass}}(t; p, \widetilde{q_-}(\epsilon)) \le \lim_{M\to\infty} f_{\text{complete}}(t; p, q, M, \alpha) \le (1-\alpha(1-\epsilon))f_{\text{Bass}}(t; p, \widetilde{q_+}(\epsilon)).$$

Letting $\epsilon \to 0$ and using (A.7) and the continuity of f_{Bass}, see (3), gives the result.

Appendix B. Dominance principle

In the heterogeneous Bass model, if j did not adopt by time t, her probability to adopt in the time interval $(t, t+\Delta t)$ is

$$\text{Prob}\begin{pmatrix} j \text{ adopts in} \\ (t, t+\Delta t)\end{pmatrix} = \Big(p_j + \sum_{i\neq j} q_{i,j} X_i(t)\Big)\Delta t, \qquad \Delta t \to 0, \tag{B.1}$$

when $X_i(t)$ is the state of consumer i, see (7), p_j describes the likelihood of j to adopt the product due to external influences, and $q_{i,j}$ describes the likelihood of j adopting the product due to internal influences by i, provided that i had already adopted the product.

Lemma 5 (*Dominance Principle [22]*). *Consider the heterogeneous Bass model (B.1) on networks A and B with M nodes, with external parameters $\{p_i^A\}$ and $\{p_i^B\}$, and with internal parameters $\{q_{i,j}^A\}$ and $\{q_{i,j}^B\}$, respectively. If*

$$p_j^A \le p_j^B \quad \text{for all } j \qquad \text{and} \qquad q_{i,j}^A \le q_{i,j}^B \quad \text{for all } i \neq j,$$

then $f_A(t) \le f_B(t)$ for $0 \le \infty$.

Appendix C. Derivation of (6c)

Following again [4, proof of Lemma 8], the evolution equation for $S^{(0)}(t; M, \alpha)$ is given by

$$\begin{aligned}\frac{\mathrm{d}}{\mathrm{d}t}S^{(0)}(t; M, \alpha) + (p+q)S^{(0)}(t; M, \alpha) = {}& \frac{q}{2}\text{Prob}\{X_{j-1}(t)=0, X_j(t)=0 \mid \widetilde{j-1}=\widetilde{j}=\widetilde{j+1}\neq\text{'r'}\} \\ & + \frac{q}{2}\text{Prob}\{X_j(t)=0, X_{j+1}(t)=0 \mid \widetilde{j-1}=\widetilde{j}=\widetilde{j+1}\neq\text{'r'}\}.\end{aligned}$$

By symmetry, both terms on the right-hand side are equal, and so

$$\frac{\mathrm{d}}{\mathrm{d}t}S^{(0)}(t; M, \alpha) + (p+q)S^{(0)}(t; M, \alpha) = q\text{Prob}\{X_j(t)=0, X_{j+1}(t)=0 \mid \widetilde{j-1}=\widetilde{j}=\widetilde{j+1}\neq\text{'r'}\}.$$

Using the conditional probabilities on the removal of node $j+2$ gives

$$\begin{aligned}&\frac{\mathrm{d}}{\mathrm{d}t}S^{(0)}(t; M, \alpha) + (p+q)S^{(0)}(t; M, \alpha) = \\ &\alpha q\text{Prob}\{X_j(t)=0, X_{j+1}(t)=0 \mid \widetilde{j-1}=\widetilde{j}=\widetilde{j+1}\neq\text{'r'},\ \widetilde{j+2}=\text{'r'}\} \\ &+ (1-\alpha)q\text{Prob}\{X_j(t)=0, X_{j+1}(t)=0 \mid \widetilde{j-1}=\widetilde{j}=\widetilde{j+1}=\widetilde{j+2}\neq\text{'r'}\}.\end{aligned} \tag{C.1}$$

By (12) and a symmetry argument,

$$\text{Prob}\{X_j(t)=0, X_{j+1}(t)=0 \mid \widetilde{j-1}=\widetilde{j}=\widetilde{j+1}\neq\text{'r'},\ \widetilde{j+2}=\text{'r'}\} = e^{-pt}S^{(1)}(t; M-1, \alpha). \tag{C.2}$$

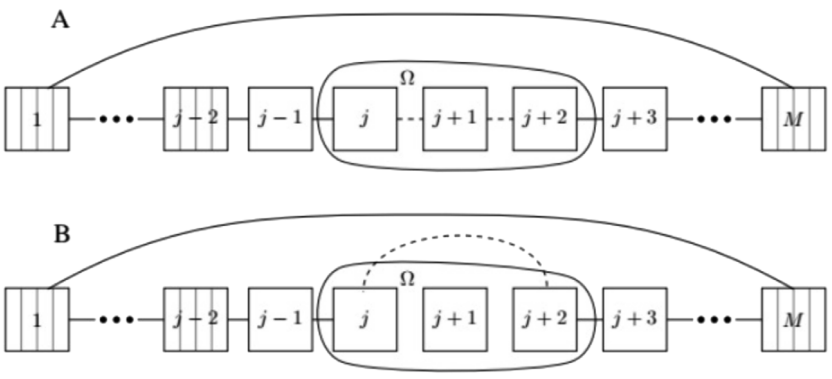

Fig. C.18. Equivalent networks for the calculation of $\text{Prob}\{X_j(t)=0, X_{j+1}(t)=0, X_{j+2}(t)=0 \mid \widetilde{j-1}=\widetilde{j}=\widetilde{j+1}=\widetilde{j+2}=\widetilde{j+3}\neq \text{`r'}\}$. Here $\Omega=\{j, j+1, j+2\}$. (A) Circular one-dimensional network, under the assumption that $\widetilde{j-1}=\widetilde{j}=\widetilde{j+1}=\widetilde{j+2}=\widetilde{j+3}\neq$ 'r'. (B) The noninfluential links from j to $j+1$ and from $j+1$ to $j+2$ are deleted. Instead, a noninfluential link that connects nodes j and $j+2$ is added.

Lemma 6.

$$\lim_{M\to\infty} Prob\{X_j(t)=0, X_{j+1}(t)=0 \mid \widetilde{j-1}=\widetilde{j}=\widetilde{j+1}=\widetilde{j+2}\neq \text{`r'}\} = \left(S_\infty^{(1)}(t;\alpha)\right)^2. \tag{C.3}$$

Proof. Let $\psi(t;M) := \text{Prob}\{X_j(t)=0, X_{j+1}(t)=0 \mid \widetilde{j-1}=\widetilde{j}=\widetilde{j+1}=\widetilde{j+2}\neq \text{`r'}\}$. Following [4, proof of Lemma 8], we obtain

$$\begin{aligned}&\frac{\mathrm{d}}{\mathrm{dt}}\psi(t;M)+(2p+q)\psi(t;M)=\\&\quad\frac{q}{2}\text{Prob}\{X_{j-1}(t)=0, X_j(t)=0, X_{j+1}(t)=0 \mid \widetilde{j-1}=\widetilde{j}=\widetilde{j+1}=\widetilde{j+2}\neq \text{`r'}\}\\&\quad+\frac{q}{2}\text{Prob}\{X_j(t)=0, X_{j+1}(t)=0, X_{j+2}(t)=0 \mid \widetilde{j-1}=\widetilde{j}=\widetilde{j+1}=\widetilde{j+2}\neq \text{`r'}\}.\end{aligned}$$

By symmetry, both terms on the right-hand side coincide, and so

$$\begin{aligned}&\frac{\mathrm{d}}{\mathrm{dt}}\psi(t;M)+(2p+q)\psi(t;M)=\\&\quad q\text{Prob}\{X_j(t)=0, X_{j+1}(t)=0, X_{j+2}(t)=0 \mid \widetilde{j-1}=\widetilde{j}=\widetilde{j+1}=\widetilde{j+2}\neq \text{`r'}\}.\end{aligned}$$

Using the conditional probabilities on the removal of node $j+3$ yields

$$\begin{aligned}&\frac{\mathrm{d}}{\mathrm{dt}}\psi(t;M)+(2p+q)\psi(t;M)=\\&\alpha q\text{Prob}\{X_j(t)=0, X_{j+1}(t)=0, X_{j+2}(t)=0 \mid \widetilde{j-1}=\widetilde{j}=\widetilde{j+1}=\widetilde{j+2}\neq \text{`r'},\ \widetilde{j+3}=\text{`r'}\}\\&+(1-\alpha)q\text{Prob}\{X_j(t)=0, X_{j+1}(t)=0, X_{j+2}(t)=0 \mid \widetilde{j-1}=\widetilde{j}=\widetilde{j+1}=\widetilde{j+2}=\widetilde{j+3}\neq \text{`r'}\}.\end{aligned} \tag{C.4}$$

By the *indifference principle*,

$$\begin{aligned}\text{Prob}\{X_j(t)=0, X_{j+1}(t)=0, X_{j+2}(t)=0 \mid \widetilde{j-1}=\widetilde{j}=\widetilde{j+1}=\widetilde{j+2}\neq \text{`r'},\ \widetilde{j+3}=\text{`r'}\} =\\ e^{-2pt}S^{(1)}(t;M-2,\alpha),\end{aligned} \tag{C.5a}$$

and

$$\text{Prob}\{X_j(t)=0, X_{j+1}(t)=0, X_{j+2}(t)=0 \mid \widetilde{j-1}=\widetilde{j}=\widetilde{j+1}=\widetilde{j+2}=\widetilde{j+3}\neq \text{`r'}\} = e^{-pt}\psi(t;M-1), \tag{C.5b}$$

see Figs. C.17 and C.18, respectively. Plugging (C.5a) and (C.5b) into (C.4), leads to the ODE

$$\frac{\mathrm{d}}{\mathrm{dt}}\psi(t;M)+(2p+q)\psi(t;M)=\alpha q e^{-2pt}S^{(1)}(t;M-2,\alpha)+(1-\alpha)qe^{-pt}\psi(t;M-1). \tag{C.6}$$

We claim that

$$\lim_{M\to\infty}\psi(M,t)=\left(S_\infty^{(1)}(t;\alpha)\right)^2. \tag{C.7}$$

Indeed, taking the limit $M\to\infty$ in (C.6) and substituting (C.7) yields the ODE (13) for $S_\infty^{(1)}(t;\alpha)$. Since in addition $\lim_{M\to\infty}\psi(0,M)=1=S_\infty^{(1)}(0,\alpha)$, the result follows.

Hence, taking the limit $M \to \infty$, and combining (C.1), (C.2) and (C.3), gives the following ODE for $S_\infty^{(0)} := \lim_{M\to\infty} S^{(0)}(t; M, \alpha)$:

$$\frac{\mathrm{d}}{\mathrm{d}t} S_\infty^{(0)}(t;\alpha) + (p+q)\, S_\infty^{(0)}(t;\alpha) = q S_\infty^{(1)}(t;\alpha)\left(\alpha e^{-pt} + (1-\alpha) S_\infty^{(1)}(t;\alpha)\right).$$

The solution of the ODE, subject to the initial condition $S_\infty^{(0)}(0;\alpha) = 1$, is given by (6c).

References

[1] E.M. Rogers, Diffusion of Innovations, Simon and Schuster, 2010.
[2] F. Bass, A new product growth model for consumer durables, Manag. Sci. 15 (1969) 1215–1227.
[3] W. Hopp, Ten most influential papers of management science's first fifty years, Manag. Sci. 50 (2004) 1763–1893.
[4] G. Fibich, R. Gibori, Aggregate diffusion dynamics in agent-based models with a spatial structure, Oper. Res. 58 (2010) 1450–1468.
[5] V. Rai, S.A. Robinson, Agent-based modeling of energy technology adoption: Empirical integration of social, behavioral, economic, and environmental factors, Enviorn. Model. Softw. 70 (2015) 163–177.
[6] V. Rai, D.C. Reeves, R. Margolis, Overcoming barriers and uncertainties in the adoption of residential solar pv, Renew. Energy 89 (2016) 498–505.
[7] K.S. Wolske, A. Todd, M. Rossol, J. McCall, B. Sigrin, Accelerating demand for residential solar photovoltaics: Can simple framing strategies increase consumer interest?, Glob. Environ. Change 53 (2018) 68–77.
[8] G.T. Kraft-Todd, B. Bollinger, K. Gillingham, S. Lamp, D.G. Rand, Credibility-enhancing displays promote the provision of non-normative public goods, Nature 563 (7730) (2018) 245.
[9] B. Bollinger, K. Gillingham, Peer effects in the diffusion of solar photovoltaic panels, Mark. Sci. 31 (2012) 900–912.
[10] M. Graziano, K. Gillingham, Spatial patterns of solar photovoltaic system adoption: The influence of neighbors and the built environment, J. Econ. Geogr. 15 (2015) 815–839.
[11] S. Solomon, G. Weisbuch, L. de Arcangelis, N. Jan, D. Stauffer, Social percolation models, Physica A 277 (2000) 239–247.
[12] G. Weisbuch, D. Stauffer, Hits and flops dynamics, Physica A 287 (2000) 563–576.
[13] J. Goldenberg, B. Libai, S. Solomon, N. Jan, D. Stauffer, Marketing percolation, Physica A 284 (2000) 335–347.
[14] S.A. Delre, W. Jager, T.H. Bijmolt, M.A. Janssen, Will it spread or not? the effects of social influences and network topology on innovation diffusion, J. Prod. Innov. Manag. 27 (2010) 267–282.
[15] M. Hohnisch, S. Pittnauer, D. Stauffer, A percolation-based model explaining delayed takeoff in new-product diffusion, Ind. Corp. Change 17 (2008) 1001–1017.
[16] S. Cantono, G. Silverberg, A percolation model of eco-innovation diffusion: the relationship between diffusion, learning economies and subsidies, Technol. Forecast. Soc. Change 76 (2009) 487–496.
[17] A.L. Barabási, Network Science, Cambridge university press, 2016.
[18] J. Goldenberg, B. Libai, E. Muller, Using complex systems analysis to advance marketing theory development: Modeling heterogeneity effects on new product growth through stochastic cellular automata, AMS Rev. 9 (2001) 1–18.
[19] R. Peres, E. Muller, V. Mahajan, Innovation diffusion and new product growth models: A critical review and research directions, Int. J. Res. Mark. 27 (2010) 91–106.
[20] G. Fibich, Bass-SIR model for diffusion of new products in social networks, Phys. Rev. E 94 (2016) 032305.
[21] S. Niu, A stochastic formulation of the bass model of new product diffusion, Math. Probl. Eng. 8 (2002) 249–263.
[22] G. Fibich, T. Levin, O. Yakir, Boundary effects in the discrete bass model, SIAM J. Appl. Math. 79 (2019) 914–937.
[23] D. Watts, S. Strogatz, Collective dynamics of 'small-world' networks, Nature 393 (1998) 440–442.
[24] A. Barabási, R. Albert, Emergence of scaling in random networks, Science 286 (1999) 509–512.
[25] B. Bollobás, O. Riordan, J. Spencer, G. Tusnády, The degree sequence of a scale-free random graph process, Random Struct. Algorithms 18 (2001) 279–290.
[26] B. Bollobás, O. Riordan, Percolation, Cambridge University Press, 2006.
[27] D. Stauffer, A. Aharony, Introduction to Percolation Theory, second ed., Taylor and Francis, London, 1994.
[28] T. Hagerup, C. Rüb, A guided tour of chernoff bounds, Inf. Process. Lett. 33 (1990) 305–308.